Automatic Geo-referencing Mobile Laser Scanning Data to UAV images

Yunlong Gao [a], Xianfeng Huang [a,*], Fan Zhang[a], Zhengwen Fu [a], Chong Yang [a]

[a] LIESMARS, Wuhan University, China - ylgao@whu.edu.cn; huangxf@whu.edu.cn; zhagnfan@whu.edu.cn; whu_fzw@163.com; yangchong609@yeah.net

3rd International Conference on Unmanned Aerial Vehicles in Geomatics
30 August-02 September 2015, York University, Canadian

KEY WORDS: Mobile Laser Scanning; UAV images; Geo-reference; Pairwise Registration; Adjustment; Trajectory

ABSTRACT:

In this paper, a framework for adjusting mobile laser scanning point cloud data to improve the accuracy is proposed by integrating high resolution UAV images and MLS. First, aerial triangulated images with a few high accuracy ground control points are taken as control information. Then, a hierarchical strategy is proposed for robust pairwise registration of feature points between point cloud and images, so as to find the deviation of the point cloud. In the next step, a shape-preserving piecewise cubic interpolating method is employed to fit the time dependent error model of the trajectory. Finally, experiments are given to prove the effectiveness of proposed framework.

1. INTRODUCTION

Recently, given the increasing need for smart city and location based services, the collection of urban spatial information and civil infrastructure modelling have become hot research topics in the photogrammetry field. Multiple sensors are employed to collect data from diverse directions to acquire more complete information. The MLS system was developed to collect high precision dense point clouds from a street view to fulfill the increasing need of street level modelling for real viewing, navigation, and location based services (Deren, 2006; Fischer and Gellersen, 2010). In addition, UAV is another very popular tool developing rapidly and used widely for collecting imageries from a top view.

The MLS is a typical survey tool that combines laser scanners, and a position and orientation unit (POS) on a mobile platform. As a combined survey system, the accuracy of points collected by MLS suffers from numerous systematic and random errors. For a well calibrated system with stable laser sensors, the accuracy of POS plays the dominant role in final data quality. Regardless of the small influences from target reflectivity properties and laser-beam incidence angle, the accuracy of platform position and orientation derived from POS determines the overall accuracies of collected data (Skaloud and Lichti, 2006). In urban area, the losing lock of GPS problem caused by dense trees, high buildings and tunnels will greatly influence the quality of mobile laser scanning data, often lasts but a short time, the shifts can reach up to meters in X,Y direction and Z direction (Haala *et al.*, 2008). Other negative factors also affect the accuracy of the GPS unit, such as a weak GPS satellite constellation, inadequate reference GPS constellations, and improper route planning. To improve the accuracy of point clouds, ground control points are surveyed manually using traditional methods and then imported to the MLS post-processing software to adjust the trajectory and point cloud, which is labour-consuming and time intensive.

UAV is a kind of popular fly platform often embedded with light sensors to collect data from an overhead view. To fulfill surveying and mapping purposes, many post-processing modules and software were developed, to process UAV data, e.g. PhotoModeler Scanner and MICMAC (Deseilligny and Clery, 2011). With the addition of high accuracy GCPs (Ground Control Points), the theoretical precision of computed object coordinates can reach centimetre accuracy (Eisenbeiss and Zhang, 2006; Nagai *et al.*, 2009).

To achieve complete data collection for urban infrastructure modelling, combining UAV images and MLS data for automatic extraction and reconstruction of urban infrastructure arouses the interest of researchers (Zhu *et al.*, 2013). Extending beyond complete model construction, integrating the two kinds of data can improve the accuracy of the acquired data. To some degree, the measured feature points from stereo UAV images can serve as control points to adjust MLS data. The two data has characteristic of compensation, UAV providing global control information which could be used to geo-reference the mobile point cloud suffering from the lost lock problem in GPS. In this paper, we propose a method to automatically geo-reference a point cloud from mobile laser scanning data by integrating it with UAV images. Our contributions are as follows:

1. A framework of adjusting mobile point clouds through UAV images automatically.
2. A hierarchical strategy for robust pairwise registration of feature points between point clouds and images.

The paper is organized as follows: the scheme for the briefly mentioned methodology is presented in detail in section 2. Section 3 presents experiments with accuracy evaluation using point cloud data from an urban environment. Conclusions and future work are given in Section 4.

* Corresponding author

2. METHOD

2.1 Method Overview

The basic assumption of our method is that the MLS data suffers from random errors of the GPS lost lock problem, UAV image could provide useful global control information to mitigate this problem. The whole procedure consists of three main phases, as shown in Figure 1. In the first phase, data pre-processing steps are performed, which include the Aero-Triangulation (AT) of UAV images based on GCPs, road area extraction from MLS data, height and intensity map interpolation. In the second phase, feature points are extracted from the road area based on intensity image, and then are registered to the UAV images by an edge-based template matching method. In the registration procedure, we propose an outlier removal method. In the third phase, a shape preservation corrected model is employed to adjust the trajectories of mobile system, which is finally used to adjust the MLS point cloud data.

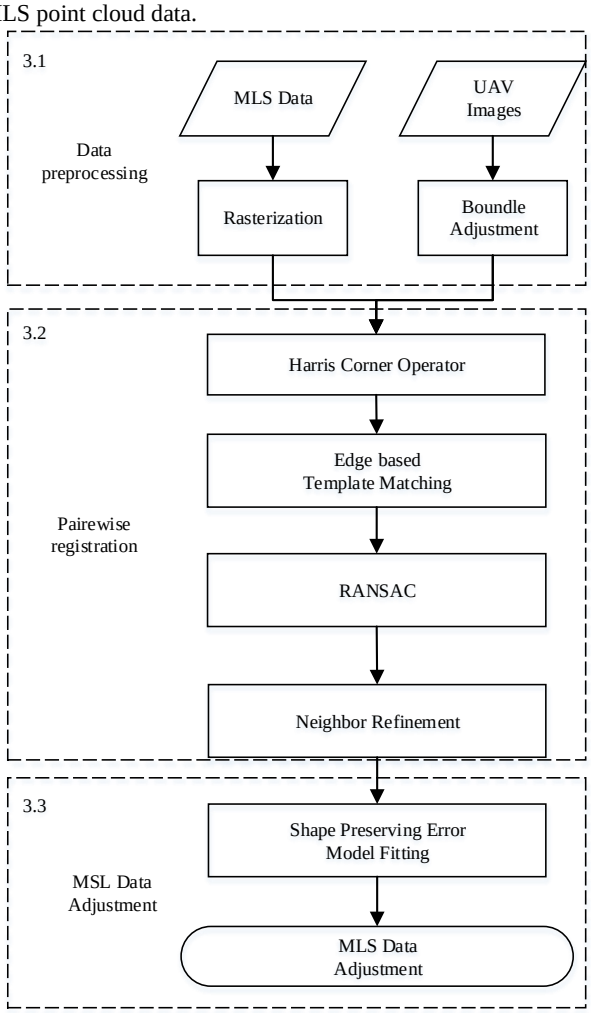

Figure 1. Processing-pipeline. Three phases: the data pre-processing of images and point clouds data, the main procedure of pairwise registration, and adjustment of the point clouds data.

2.2 Data Pre-processing

Before data adjustment, the given MLS data and UAV data needs pre-processing. A MLS point cloud is subdivided into blocks, such as 80 * 80 meters. The pre-processing procedure contains three steps: road extraction from MLS point cloud, intensity interpolation and UAV images aerial triangulation.

a) Road point extraction from MLS point cloud data. Road markings are always very clear and can be identified from the background in both MLS point cloud intensity data and UAV images. With sharp corners and strong colour contrast, road markings have reliable and stable corner point features to establish corresponding relationships between the ground and aerial observations. To extract road marking corner points from MLS intensity data, a filter algorithm is applied to remove non-terrain points. In our experiment, we assumed that the trajectory of MLS system has a very stable relative height to the road, or the "ground". Based on this assumption, the average height of neighbouring nodes of trajectory are taken as a threshold, points with timestamps between the nodal timestamp above the threshold will be removed.

b) Interpolation of point cloud intensity data. To simplify the processing, the intensity information of unstructured point cloud should be interpolated into raster maps (Poullis, 2013). We employ the resolution of the intensity map as 0.04m, which corresponds to the average MLS data point cloud density of interesting area and represent more accuracy of single point information. For each block of 80m*80m, the intensity map $I_{xy} = \{i|(x,y)\}$ has 2000*2000 pixels. The height map $Z_{xy} = \{z|(x,y)\}$ is interpolated by the same method.

c) Aerial Triangulation of UAV images
The camera of the UAV is calibrated using *IWitness* software (Fraser and Hanley, 2004). The precise exterior orientation parameters for aerial images are obtained by *MICMAC*, an open source bundle adjustment software for automatic camera calibration and orientation of set of images, developed by IGN (Deseilligny and Clery, 2011).

2.3 Pairwise registration of UAV images and point cloud

2.3.1 Feature point extraction. Before the corresponding points finding between MLS to UAV images, seed points are extracted. The Harris operator is a classic and efficient corner detector, widely used for detecting corner points in image matching and registration (Yu *et al.*, 2008). The intensity image is interpolated and an improved Harris operator (Zhu and Wu, 2007) is applying to detect corner points. The detection result is shown as Figure 2.

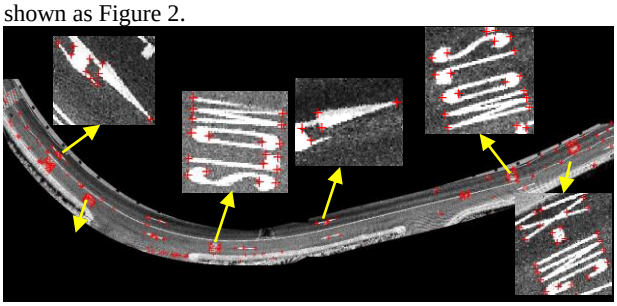

Figure 2. Feature points detected by the Harris operator from the intensity image. Red-crosses are the detected corner points, though there are many random noises in the intensity image.

We must notice that the image characteristics of road marks in point cloud intensity data have intrinsic differences to that in the UAV images. The intensity value represents the received energy of laser beam reflection and UAV image record the reflection of nature visible light with diffusion effect by camera CCD. From a visual perspective, the edge of road marks of intensity data and UAV image are very clear and similar. Thus, we employ edges as the cues to instead corner to corner matching results.

2.3.2 Point matching using a local template. Edges in our method are extracted by classic Canny edge detector (Canny, 1986). For processing edge based template matching, a new method is presented using distance and density to measure spatial and probabilistic distribution similarities. Given a seed point $p(X_i, Y_i)$, a small template image is firstly cropped from the intensity edge image with predefined window size. Then, we try to find the corresponding points from UAV images.

Given a seed point $q(x_i, y_i)$ in an intensity image I with m relative UAV images $J = \{I_j | j = 1,2, \dots m\}$, a corresponding $p(X_i, Y_i, Z_i)$ from the intensity image can be computed with the help of height map. Since each image has its position and orientation parameters, we can find serial points $q(x_i^j, y_i^j), j = 1,2, \dots, M$ from the relative image group J by ground point $p(X_i, Y_i, Z_i)$ with the help of photogrammetric collinear equation. Then the point sets $q(x_i^j, y_i^j), j = 1,2, \dots, M$ are taken as candidate points group to match the ground seed points. For each point, a small image block is cropped from the UAV and intensity images, thus multiple stereo images are involved in seed point matching using this procedure.

For each matching step, the centre of the template is simply moved over the matching image and the acceptability value is computed. The whole procedure for the template matching process is shown as Figure 3. In the first row of Figure 3-(a) is the template intensity image with a seed point in a cross marker and related searching UAV images with a corresponding projection marker. After edge detection process by Canny edge detector, Figure 3-(b) shows the corresponding edge images. Based on the edge template matching, Figure 3-(c) shows the template edge results in red over the searched images. Based on our method, the tie point matching results are shown as Figure 3-(d) with a red marker.

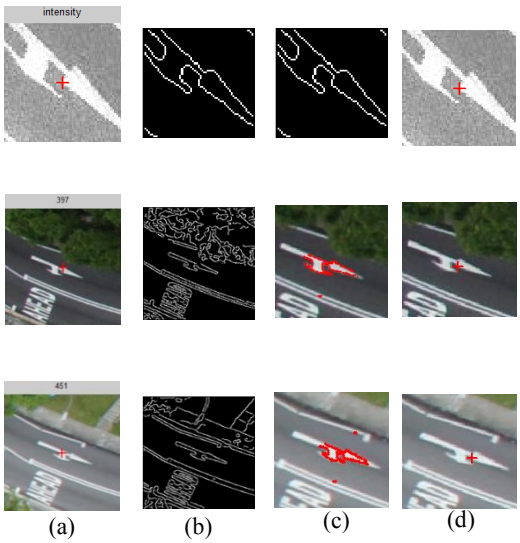

Figure 3. The procedure of template matching.

2.3.3 Outlier removal. For all matched point pairs, a MLS feature point $p(X_i, Y_i)$ is observed by multiple images with corresponding points $q(x_i^k, y_i^k), k = 1,2, \dots K$ in image coordinate space. Due to the inevitable occurrence of mismatches, RANSAC algorithm (Fischler and Bolles, 1981) is introduced to remove the outliers from matching results.

The basic idea of the RANSAC outlier removing procedure is illustrated as Figure 4. Firstly, we pick two images and corresponding tie points randomly. Using the orientation information from the selected images and tie points, a ground point G is computed based on a forward intersection. Next, a reverse projection from G to the remaining image is performed to compute bias t_i, which is the Euclidean distance between the projected point (spot marker) and matched point (cross marker) in pixels. The details steps are listed below:

1. Randomly choosing a pair of $q(x_i^k, y_i^k), k = 1,2, \dots K$.
2. Generating the solution of forward intersection based on related orientation information and the chosen pair.
3. Taking the solution as ground point and the orientation information of each, a new point in each image space is computed with collinear equation corresponding to the matched point.
4. Comparing with the given threshold, the difference of the new point and matched point is accepted or rejected as an inlier and outlier.
5. The process will repeat from step one to four until the previously set conditions are satisfied.
6. Finally, the solution is output as a ground point (X_i', Y_i', Z_i') fitted by least mean square method. In addition, the outlier removing processing converts the points from image coordinates to geometric coordinates.

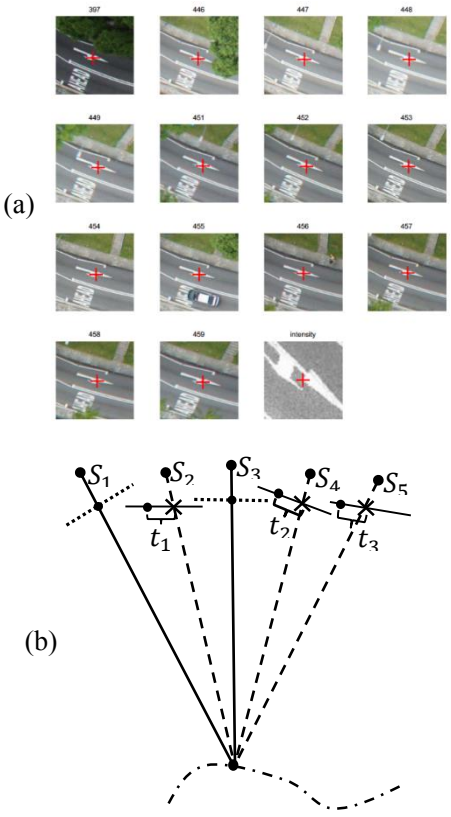

Figure 4. (a) shows the result of template matching as tie points between the intensity map (the last one) and UAV images with the cross marker. (b) illustrates the RANSAC procedure based on the result of template matching. G represents a ground point with chosen image S_1 and S_3. $t_i, \mathrm{i} = 1,2,3$ is the difference of a spot representing matched point and a cross representing the computed in S_2, S_4, S_5 respectively.

2.3.4 Point cloud adjustment. The errors of the position observations of the POS system are time dependent (Zhang et. al., 2012). From the LiDAR geo-reference equation, the coordinate bias $[\Delta x, \Delta y, \Delta z]$ of a point is decided mainly by POS error. After outlier removal processing, a set of matched point pairs is acquired which contain the coordinate bias at a certain time.

These points, which will be used as the key points for point cloud adjustment, allocate along the trajectory of MLS system with a non-uniform distributions. Each point represents a point with independent deviation vector. That means a smooth interpolation function is needed to adjust the point cloud. In this paper, we introduce a Shape-Preserving Piecewise Cubic Hermite Interpolating (SPPCHI) method to generate smooth trajectory adjustment parameters, originally proposed by (Delbourgo and Gregory, 1985). SPPCHI is a first order approximation accuracy interpolation method and its interpolation values between the maximum and minimum of nodes are more stable as compared to the traditional high degree polynomial function. The error model function of time is generated in the X, Y *and* Z directions separately. Knowing the value of GPS time stamp t, the position observation error of each point $(\Delta X(t), \Delta Y(t), \Delta Z(t))$ can be computed out. Thus, the new point coordinate $(X'(t), Y'(t), Z'(t))$ after correcting can be computed using formula:

$$\begin{cases} X'(t) = X(t) + \Delta X(t) \\ Y'(t) = Y(t) + \Delta Y(t) \\ Z'(t) = Z(t) + \Delta Z(t) \end{cases} \quad (1)$$

Where $X(t)$ is the original coordinate in X direction at time t. $\Delta X(t)$ and $X'(t)$ are the correction and the new point. For the Y and Z direction, the processing steps are similar.

3. EXPERIMENT

3.1 Test Data

The experimental data was collected in 2012 at the National University of Singapore (NUS) with high buildings and dense trees. The data includes both a MLS point cloud and aerial images from UAV. The point cloud data set was obtained by the RIEGL VMX 250 system with two VQ-250 laser scanners. The area of an 80m*80m data block was interpolated into 2000*2000 image using an average 0.04 meter grid size, which means the entire range and intensity of values of each point was preserved with very little loss of information from rasterization. Figure.5 shows the whole test area and a part of the intensity map.

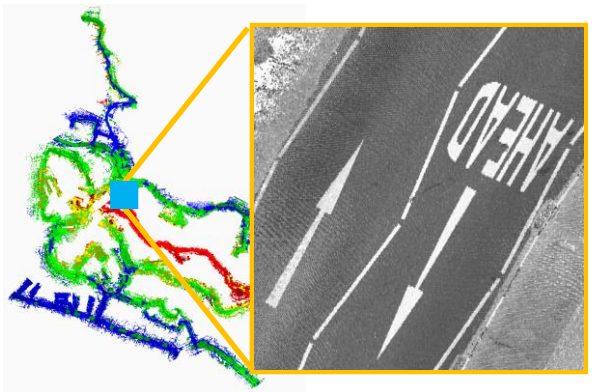

Figure 5 shows the overview of point cloud data in NUS. Right figure is the interpolated intensity image, which shows very clear land marks.

The corresponding aerial images were collected using the AscTec Falcon 8 octocopter system with an off-the-shelf camera Sony Nex-5. After data cleaning, 787 of 857 images are selected to be test data, depicted in Figure 6 left as green. The average flight height was 120 m and the average ground resolution was about 0.05m. Bundle adjustment was conducted based on 23 of total 34 ground control points surveyed using GPS with around 0.02m accuracy. The rest 11 control points were used as check points to evaluate the bundle adjustment accuracy. The RMSE of coordinate residues of the check points was 0.046m, 0.053m in X, Y direction and 0.093m in the Z direction, as shown in Figure 6 right.

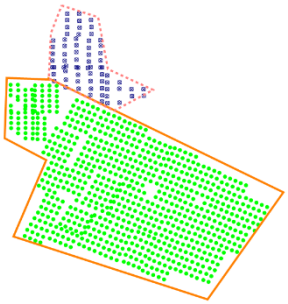

Pt	ResX(m)	ResY(m)	ResZ(m)
1	0.047	0.032	-0.136
2	-0.051	-0.067	-0.095
3	-0.081	0.032	-0.102
4	0.065	-0.123	-0.083
5	0.03	-0.010	-0.059
6	0.016	0.021	-0.032
7	-0.054	-0.025	0.0610
8	0.03	0.08	0.094
9	-0.028	-0.019	-0.044
10	-0.014	-0.025	0.110
11	0.047	0.032	-0.137
RMSE	0.046	0.053	0.093

Figure 6. The left is the layout of the whole NUS image blocks. The right shows the residual of check points after Bundle Adjustment.

3.2 Data Adjustment

After pairwise registration, the position deviation of each point were acquired in X, Y and Z directions. According to the approach detailed in section 2.4, the trajectory was adjusted by SPPCHI using the detected biases points. Then, the new trajectory was used as the source for the point cloud adjustment procedure. According equation (1), new coordinates were computed and assigned to each point. The difference of the trajectory before and after interpolation is shown in Figure 7. The colour difference denotes different trajectory deviation values. In this figure, we see that GPS inaccuracy happens very often along the trajectory. In this experiment, the deviations were smaller than 0.7m in most areas, but there are many areas bigger than 1.0 meters, especially the areas with high buildings and dense trees.

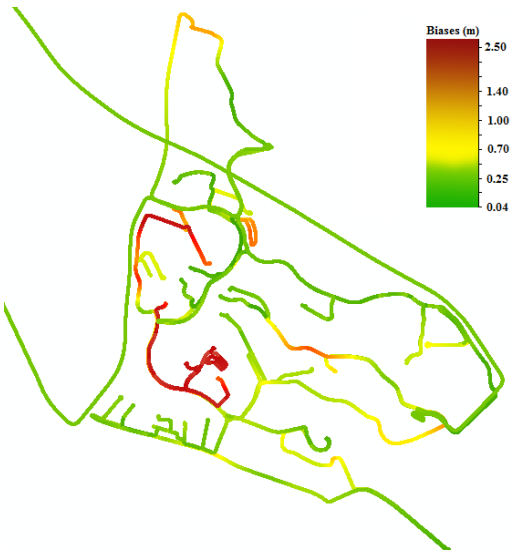

Figure 7. The new trajectory coloured by the magnitude of the sum of X, Y and Z direction.

3.3 Accuracy Evaluation

To evaluate the accuracy of the processed data, a few uniformly distributed check points were selected manually from the original point clouds data set using TerraScan software, as well as corresponding points in corrected data. Control points are measured manually using LPS software from UAV stereo images with AT processing. The root mean square value of the differences between check points and control points is calculated before and after the trajectory correction.

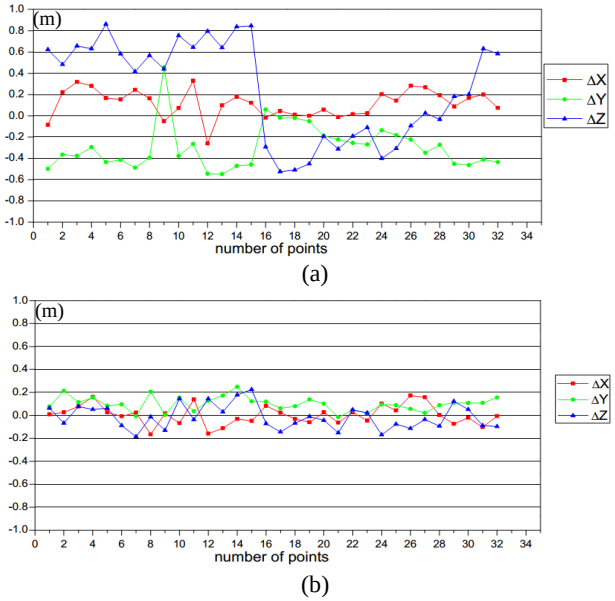

Figure 8. (a) Differences between control points and check points for the unadjusted data (RMS-ΔX=**0.130m**, RMS-ΔY=**0.211m**, RMS-ΔZ=**0.467m**). (b) Difference between control point and check point from corrected data (RMS-ΔX=**0.086m**, RMS-ΔY=**0.063m**, RMS-ΔZ=**0.106m**).

Figure 8-(a) shows the differences between check points and control points from the unadjusted data. It is very clear that there are some points of big differences. The vertical variance (0.467m) is rather higher than the horizontal variance (0.130m and 0.211m), consistent with RTK surveying experience where the precision of the vertical is double the precision of position obtained by the RTK system. Figure 8-(b) shows the results after point cloud correction. The variance of position of check points in the X and Y direction are 0.086m and 0.063m, in the vertical direction about 0.106m. It greatly improved the quality of original point cloud without spending much labour and time on GPS survey field work. This procedure can automatically register the original point cloud to the UAV images, providing a good basis for future complete modelling processing.

4. CONCLUSION

In this paper, we propose a novel framework to automatically geo-reference MLS point clouds to UAV data, which can improve the accuracy of MLS point cloud data. In the proposed method, all the extracted corresponding feature points on white road markings are processed robustly to guarantee the quality of extracted control points using a hierarchical strategy. The experimental results of registration demonstrate that the proposed method is practical for urban area data registration using road markings between images and point clouds. Another benefit of our work is that it reduces labour intensive field work of control point surveying. In MLS surveying for dense urban areas, the average distance between two control points is typically about 100~200 meters. Thus, only a few control points are needed to adjust the MLS point cloud using UAV images, rather than a hundred control points along the road, collected under field conditions.

The robustness of our proposed automatic method depends on the control point matching results. If the feature differences between an image and intensity map are too large to obtain satisfactory point matching results, the robustness of our method will be influenced. Undoubtedly, such a procedure could improve the quality of data. But, by addressing the symptoms of problem rather than its cause, does not allow one to fully realize model accuracy in MLS system technology.

ACKNOWLEDGEMENTS (OPTIONAL)

The authors would greatly thank Prof. Armin Gruen and the Future Cities Laboratory (FCL) of Singapore-ETH Centre for providing the test data set and many valuable help. The authors conceived this idea during working period in FCL under the supervising of Prof. Armin Gruen, and developed it in Wuhan University.

This research was supported by the National Basic Research Program of China (No. 2012CB725300), National Key Technology Support Program of China (No. 2012BAH43F02).

REFERENCES

Canny, J., 1986. A computational approach to edge detection, *Pattern Analysis and Machine Intelligence, IEEE Transactions on*, PAMI-8(6):679-698.

Delbourgo, R., and J. Gregory, 1985. Shape preserving piecewise rational interpolation, *SIAM journal on scientific and statistical computing*, 6(4):967-976.

Deren, L., 2006. Mobile mapping technology and its applications [j], *Geospatial Information*, 4(4):125.

Deseilligny, M.P., and I. Clery, Apero, an open source bundle adjusment software for automatic calibration and orientation of set of images, *Proceedings of the ISPRS Symposium, 3DARCH11*, 2011.

Eisenbeiss, H., and L. Zhang, 2006. Comparison of dsms generated from mini uav imagery and terrestrial laser scanner in a cultural heritage application, *International Archives of Photogrammetry, Remote Sensing and Spatial Information Sciences XXXVI-5, 90e96*.

Fischer, C., and H. Gellersen, 2010. Location and navigation support for emergency responders: A survey, *IEEE Pervasive Computing*, 9(1):38-47.

Fischler, M.A., and R.C. Bolles, 1981. Random sample consensus: A paradigm for model fitting with applications to image analysis and automated cartography, *Communications of the ACM*, 24(6):381-395.

Fraser, C., and H. Hanley, Developments in close-range photogrammetry for 3d modelling: The iwitness example, *Presented paper, International Workshop: Processing and Visualization using High-Resolution Imagery, Pitsanulok*, 2004.

Gruen, A., X. Huang, R. Qin, T. Du, W. Fang, J. Boavida, and A. Oliveira, 2013. Joint processing of uav imagery and terrestrial mobile mapping system data for very high resolution city

modeling, *ISPRS-International Archives of the Photogrammetry, Remote Sensing and Spatial Information Sciences*, 1(2):175-182.

Haala, N., M. Peter, J. Kremer, and G. Hunter, 2008. Mobile lidar mapping for 3d point cloud collection in urban areas-a performance test, *The International Archives of the Photogrammetry, Remote Sensing and Spatial Information Sciences*, 37:1119-1127.

Nagai, M., T. Chen, R. Shibasaki, H. Kumagai, and A. Ahmed, 2009. Uav-borne 3-d mapping system by multisensor integration, *Geoscience and Remote Sensing, IEEE Transactions on*, 47(3):701-708.

Poullis, C., 2013. A framework for automatic modeling from point cloud data, *Pattern Analysis and Machine Intelligence, IEEE Transactions on*, 35(11):2563-2575.

Puente, I., H. González-Jorge, B. Riveiro, and P. Arias, 2012. Accuracy verification of the lynx mobile mapper system, *Optics & Laser Technology*.

Skaloud, J., and D. Lichti, 2006. Rigorous approach to bore-sight self-calibration in airborne laser scanning, *ISPRS Journal of Photogrammetry and Remote Sensing*, 61(1):47-59.

Yu, L., D. Zhang, and E.-J. Holden, 2008. A fast and fully automatic registration approach based on point features for multi-source remote-sensing images, *Computers & Geosciences*, 34(7):838-848.

Zhu, L., A. Jaakkola, and J. Hyyppä, 2013. The use of mobile laser scanning data and unmanned aerial vehicle images for 3d model reconstruction.